PHYSICAL REVIEW A VOLUME 32, NUMBER 5 NOVEMBER 1985

Optical-potential model for electron-atom scattering

Joseph Callaway and D. H. Oza
Department of Physics and Astronomy, Louisiana State University, Baton Rouge, Louisiana 70803-4001
(Received 12 July 1985)

It is proposed that the addition of a matrix optical potential to a close-coupling calculation should lead to improved results in studies of electron-atom scattering. This procedure is described with use of a pseudostate expansion to evaluate the optical potential. The integro-differential equations are solved by a linear-algebraic method. As a test case, applications are made to electron-hydrogen scattering, and the results are compared with those obtained by other calculational procedures, and with experiment.

I. INTRODUCTION

The optical-potential approach arises in a natural way as an extension of the close-coupling approach to electron-atom scattering at intermediate energies. We focus our attention on the description of the excitation of a discrete state for electron impact energies at which many other channels are open. If the incident energy is greater than the lowest ionization potential, an infinite number of channels will be open. It is not possible to include the large number of (all) open channels explicitly in a close-coupling calculation. It becomes necessary to adopt a procedure in which the effect on a specific transition of processes involving other channels too numerous for explicit treatment can be included. This is done through the development of an optical potential.

Optical-potential methods in the theory atomic scattering have been extensively developed and employed by Bransden and McCarthy and their collaborators.[1–6] References to earlier work and to other authors can be found in Ref. 7.

The essential ideas of this approach can be qualitatively presented as follows (a more formal treatment is given in Sec. II). Certain channels are selected in which we are specifically interested; perhaps only one if we are concerned with elastic scattering, or a few if we want to describe some excitations. The infinite set of coupled integro-differential equations of the close coupling method are partitioned into two groups P and Q. The P group describes those channels we wish to consider explicitly; the more numerous Q set contains the rest. The equations for the Q set are solved formally by a Green's-function technique in a manner which relates the solution for the Q to those for the P. At this point, one normally introduces an approximation which is practically necessary although not formally required, of neglecting the coupling of the channels in the Q set with each other (the coupling of Q to P is, however, essential). The resulting formal solution for the Q set is substituted into the equations for the P set, which then contains nonlocal, energy-dependent, complex terms we describe as the optical potential. It is useful to observe that in the low-energy limit for elastic scattering, the optical potential reduces to the ordinary polarization potential (with nonadiabatic and energy-dependent corrections).

This approach ought to be generally applicable in the intermediate energy range; i.e., in that regime of electron incident energies above the first ionization threshold but insufficiently large to permit accurate application of high-energy (Born, Glauber, etc.). In addition, it should be possible to treat the problem of elastic scattering from excited states, which is important in the determination of the widths and shifts of spectral lines in astrophysical and low-density laboratory plasmas. This problem acquires its complexity from the large number of channels accessible with relatively low incident energies.

In general, we think it is useful to regard the optical potential approach as an approximation. Given a sufficiently fast and large (in memory) computer, one could solve the scattering problem through a close-coupling expansion involving many pseudostates in sufficient detail to permit accurate extraction of amplitudes in the presence of pseudothreshold structure by T matrix fitting.[8] At present it is only in the case of the electron-hydrogen system that results of this sort are available.[9] Use of the optical potential in the manner described here omits the detailed dynamics associated with the coupling of the pseudostates with each other. However, we shall see that in the case of elastic scattering, excellent agreement is obtained with more comprehensive calculations without the need to resort to a fitting process to suppress pseudoresonances. In the case of excitation, the present results, though not as satisfactory as in the case of elastic scattering, clearly go a long way toward correcting the errors of a limited basis close-coupling calculation.

This paper describes our initial efforts to implement this procedure. The optical potential is constructed using a set of pseudostates to enable evaluation of the sum over intermediate states.[2] After the optical potential has been constructed, it is necessary to solve the remaining integro-differential equations in the P space. We have chosen for this purpose a linear-algebraic integral-equation method[10,11] supplemented by an asymptotic K-matrix propagation procedure in the asymptotic region.[12] The formal theory of the optical potential is described in Sec. II. Our numerical methods are discussed briefly in Sec. III. Section IV contains the pseudostate basis. Specific numerical results for the test case of electron-hydrogen

scattering are presented in Sec. V. These results emphasize elastic scattering by the atomic ground state. We compare our results with measurements of differential cross sections,[13] and with recent measurements of the spin asymmetry at 90° in elastic scattering.[14] Finally, a summary of this work and our conclusions are presented in Sec. VI.

II. THEORY

In order to establish the notation, we first review briefly the derivation of the fundamental integro-differential equations. We then introduce the optical potential, and describe how it is to be computed, allowing for both closed and open pseudochannels. Finally, we describe the linear-algebraic method which is to be used to solve the coupled integrodifferential equations.

For simplicity we consider a target atom (or ion) of nuclear charge Z with one electron. The formal generalization to more complex targets is, we believe, rather obvious. Let $\mathbf{r}$ denote the coordinates of the scattering electron and $\mathbf{x}$ that of atomic electron, both with respect to the atomic nucleus as origin. $\Psi_a(\mathbf{r},\mathbf{x})$ is a wave function obeying the K-matrix boundary condition in which there is an incident particle in channel a only. Conserved quantum numbers (L,S,Π—total angular momentum, total spin, and parity) are implied. This function is to be expanded in a complete set of states (atomic functions supplemented by pseudostates) for the target atom; multiplied by scattering functions to be determined for the projectile:

$$\Psi_a(\mathbf{r},\mathbf{x})=[1+(-1)^S P_{12}] \times \sum_j \phi_{ja}(r)u_j(x)Y^{M\pi}_{Ll_1'l_2'}(\hat{\mathbf{r}}_1,\hat{\mathbf{r}}_2) . \tag{2.1}$$

In this equation, $Y^{M\Pi}_{Ll_1'l_2'}$ is a two-particle spherical harmonic for total angular momentum L (z component M, parity Π) while l_1' and l_2' are the individual angular momenta. We associate l_1' with $\hat{\mathbf{r}}_1$ and l_2' with $\hat{\mathbf{x}}$. The function $u_j(x)$ is a member of the complete set of states describing the target for angular momentum l_2', and $\phi_{ja}(r)$ is the corresponding radial scattering function. The index j on ϕ includes all the quantum numbers required to specify a channel. The sum includes the partial angular momenta l_1' and and l_2' and the indices of the target states.

The functions $u_j(x)$ are supposed to diagonalize the Hamiltonian of the target H_T,

$$\int d^3x\, u_k^*(x)Y^*_{l_km_k}(\hat{\mathbf{x}})H_T(x)u_j(x)Y_{l_jm_j}(\hat{\mathbf{x}})=E_j\delta_{jk} . \tag{2.2}$$

If the set of states used in (1) were complete, Eq. (2) implies that they would be the exact eigenfunctions of the target Hamiltonian. We require that Eq. (2) must be exactly satisfied for whatever finite set of target states is actually used. The set of functions u then usually contains both exact and approximate target states (or pseudostates).

The Hamiltonian for the scattering problem is

$$H(\mathbf{r},\mathbf{x})=H_T(\mathbf{r})+H_T(\mathbf{x})+\frac{e^2}{|\mathbf{r}-\mathbf{x}|} , \tag{2.3a}$$

where

$$H_T(\mathbf{r})=-\nabla_{\mathbf{r}}^2+\frac{Ze^2}{r} \tag{2.3b}$$

(and Z is the nuclear charge).

The equations for the functions ϕ_{ja} are obtained by requiring that the Schrödinger equation should be exactly satisfied in that part of function space spanned by the target functions. Specifically, we have

$$\int u_i^*(x)Y^{M\Pi}_{Ll_1l_2}(\hat{\mathbf{r}},\hat{\mathbf{x}})[H(\mathbf{r},\mathbf{x})-E]\Psi_a(\mathbf{r},\mathbf{x})d\hat{\mathbf{r}}\,d^3x=0 . \tag{2.4}$$

After a considerable amount of algebraic manipulations, we obtain equations for the ϕ_{ja} which can be put in the following form:

$$(H_{l_1}-k_i^2)\phi_{ia}(r)+\sum_j \int dx\, x^2K_{ij}(r,x)\phi_{ja}(x)=0 , \tag{2.5}$$

in which H_{l_1} is the radial Hamiltonian for angular momentum l_1

$$H_{l_1}=-\frac{1}{r^2}\frac{d}{dr}\left[r^2\frac{d}{dr}\right]+\frac{l_1(l_1+1)}{r^2}-\frac{(Z-1)e^2}{r} \tag{2.6}$$

and K_{ij} (the "kernel") is an operator containing both direct (local) and exchange (nonlocal) contributions

$$K_{ij}(r,x) = \left[V_{ij}(r)-\frac{e^2}{r}\delta_{ij}\right]\frac{\delta(r-x)}{r^2} + (-1)^S u_i^*(x)[W_{ij}(x,r)-(k_i^2-E_j)\delta_{l_1l_1'}\delta_{l_2l_2'}]u_j(r) . \tag{2.7}$$

In these expressions

$$k_i^2=E-E_i , \tag{2.8a}$$

$$V_{ij}(r)=\int d^3x\, d\hat{\mathbf{r}}\, u_i(x)[Y^{M\Pi}_{Ll_1l_2}(\hat{\mathbf{r}},\hat{\mathbf{x}})]^*\frac{e^2}{|\mathbf{r}-\mathbf{x}|}u_j(x) \times Y^{M\Pi}_{Ll_1l_2}(\hat{\mathbf{x}},\hat{\mathbf{r}}) . \tag{2.8b}$$

We shall refer to V_{ij} as the direct potential (matrix) and W_{ij} as the exchange potential (matrix). The angular integrations can be performed according to Percival and Seaton.[15] This leads to

$$V_{ij}(r)=\sum_\lambda Q(L,l_1,l_2,l_1',l_2',\lambda)y_{ij}^{(\lambda)}(r) , \tag{2.9a}$$

$$W_{ij}(x,r)=e^2\sum_\lambda Q(L,l_1,l_2,l_2',l_1',\lambda)r_<^\lambda/r_>^{\lambda+1} , \tag{2.9b}$$

in which $r_<$ is the lesser and $r_>$ the greater of x and r; $y_{ij}^{(\lambda)}$ is given by

$$y_{ij}^{(\lambda)}(r)=\frac{e^2}{r^{\lambda+1}}\int_0^r u_i^*(x)x^{\lambda+2}u_j(x)dx + e^2r^\lambda\int_r^\infty \frac{u_i^*(x)u_j(x)}{x^{\lambda-1}}dx , \tag{2.10}$$

and Q is a coefficient whose general expression is

$$Q(L,l_1,l_2,l_1',l_2',\lambda)=(-1)^{l_1+l_1'-L}[(2l_1+1)(2l_2+1)(2l_1'+1)(2l_2'+1)]^{1/2} \times \begin{bmatrix} l_1' & \lambda & l_1 \\ 0 & 0 & 0 \end{bmatrix} \begin{bmatrix} l_2' & \lambda & l_2 \\ 0 & 0 & 0 \end{bmatrix} \begin{Bmatrix} L & l_2 & l_1 \\ \lambda & l_1' & l_2' \end{Bmatrix}, \tag{2.11}$$

and the standard notation for the 3-j and 6-j symbols has been used.

We are now ready to introduce the optical potential. For this purpose we separate the set of channels considered into two groups: Set 1, those to be considered explicitly (the P space). These channels have indices in the range of j from j_0 to j_1, and the sum over channels in this set will be denoted $\sum_P$. Set 2 (the Q space) comprises all other channels, and the sum over these is denoted $\sum_Q$. Consider now Eq. (2.5). Suppose i is a channel in set 2. We approximate Eq. (2.5) by restricting the sum over j to channels in set 1. Equation (2.5) is then an inhomogeneous equation, which is solved by introducing the Green's function, $\gamma_i(r,y)$, which satisfies

$$(H_{l_1}-k_i^2)\gamma_i(r,y)\frac{1}{y^2}\delta(r-y) . \tag{2.12}$$

Then we have

$$\phi_{ia}(r)=-\sum_{j\in P}\int dy\, y^2 \int dx\, x^2\gamma_i(r,y)K_{ij}(y,x)\phi_{ja}(x) . \tag{2.13}$$

We now return to Eq. (2.5) for the case in which i is in set 1. In this case we separate the sum over channels into the part involving the P and Q subspaces, and use Eq. (2.13) for those channels which belong to Q. The result is an equation (or a set of coupled equations) restricted to the P space:

$$(H_{l_1}-k_i^2)\phi_{ia}(r) + \sum_{j\in P}\int dx\, \psi^2[K_{ij}(r,x)+U_{ij}(r,x)]\phi_{ja}(x)=0 , \tag{2.14}$$

in which

$$U_{ij}(r,x)=-\sum_{m\in Q}\int y^2dy \int z^2dz\, K_{im}(r,y) \times\gamma_m(y,z)K_{mj}(z,x) . \tag{2.15}$$

The quantities U_{ij} define the optical potential.

Approximations are generally necessary in the construction of the optical potential. The most usual of these is the neglect of exchange in the matrix elements between the P and Q spaces; i.e., in Eq. (2.15) put

$$K_{im}(r,y)=V_{im}(r)\frac{\delta(r-y)}{y^2} .$$

Then U_{ij} reduces to

$$U_{ij}(r,x)=-\sum_{m\in Q}V_{im}(r)\gamma_m(r-x)V_{mj}(x) . \tag{2.16}$$

Equations (2.14) and (2.16) are the equations to be solved in this work.

The calculation of the optical potential requires the Green's function γ_m. Since H_l as defined in Eq. (6) contains only a pure Coulomb potential, γ_m can be specified analytically. The direct diagonal potential element V_{mm} could be included in the calculation of γ_m without any change in the formalism, but then γ_m would have to be found by numerical solution of a differential equation, and the calculation would be much slower.

Let $F_l(k_mr)$ be a regular Coulomb wave function with the asymptotic form

$$F_l(kr)\rightarrow\sin\theta_l , \tag{2.17a}$$

where

$$\theta_l=kr+(Z-1)\ln(2kr)-\frac{l\pi}{2}+\sigma_l \tag{2.17b}$$

(σ_l is the Coulomb phase), and let G_l be an irregular solution

$$G_l(kr)\rightarrow\cos\theta_l . \tag{2.17c}$$

(If V_{mm} is included, the asymptotic forms are unchanged.) In the case of a neutral system, the logarithmic term and σ_l do not appear, and the Coulomb functions become Bessel functions. The Green's function appropriate for use in (2.16) is

$$\gamma_m(r,x)=\frac{1}{k_m}\frac{F_l(k_mr_<)}{rx}[G_l(k_mr_>)+iF_l(k_mr_>)] . \tag{2.18}$$

For $k_m^2<0$, negative energy Coulomb wave functions are required. Let these be denoted f_l and g_l for the regular and irregular cases. We define new function x_1 and x_2 by

$$\begin{bmatrix} f_l \\ g_l \end{bmatrix}=r^{l+1}e^{-\kappa r}\begin{bmatrix} \chi_1 \\ \chi_2 \end{bmatrix} , \tag{2.19a}$$

where $\kappa^2=-k_m^2$. Then χ_1 may be chosen to be the regular confluent hypergeometric function,

$$\chi_1(r)={}_1F_1(l+1-Z/\kappa,2l+2,2\kappa r) , \tag{2.19b}$$

and χ_2 is the irregular function

$$\chi_2=U(l+1-Z/\kappa,2l+2,2\kappa r) . \tag{2.19c}$$

The Green's function is proportional to the product f_lg_l:

$$\gamma(r,x)=\frac{A(\kappa,l)}{rx}f_l(r_<)g_l(r_>) . \tag{2.20}$$

The constant of proportionality is determined from the Wronskian of f_l and g_l, which can be evaluated using the asymptotic forms of the functions. The result is

$$A(\kappa,l)=-(2\kappa)^{2l+1}\frac{\Gamma(l+1-Z/\kappa)}{\Gamma(2l+2)} . \tag{2.21}$$

Finally we consider the linear-algebraic method employed for the solutions of the coupled set of Eq. (2.14). As a result of the previous considerations, the channels explicitly considered are restricted to the P space, and the kernel K is a nonlocal, energy-dependent quantity.

In the linear-algebraic method,[11] we convert the integro-differential equations into integral equations by introducing the appropriate Green's function. Only (some of the) open channels are explicitly considered. The Green's function, denoted Ω, to be employed is similar to that of Eq. (18) except that it is convenient to employ K-matrix boundary conditions, even though the K matrix is complex, in consequence of the use of a complex optical potential. Thus

$$\Omega_i(r,x)=\frac{1}{k_i}\frac{F_{l_1}(k_i r_<)G_{l_1}(k_i r_>)}{rx} . \tag{2.22}$$

Then we find

$$\phi_{ia}(r)=\frac{1}{r}F_{l_1}(k_i r)\delta_{ia}-\sum_{j\in P}\int \Omega_j(r,x)\left[[V_{ij}(x)-(e^2/r)\delta_{ij}]\phi_{ja}(x)+\int y^2[u_i(y)W'_{ij}(y,x)u_j(x)+U_{ij}(x,y)]\phi_{ja}(y)\right]x^2\,dx , \tag{2.23}$$

in which Eq. (2.7) has been used, and for simplicity of notation we have included the term $(k_i^2-E_j)$ in the definition of W'_{ij},

$$W'_{ij}(y,x)=W_{ij}(y,x)-(k_i^2-E_j)\delta_{l_1l'_2}\delta_{l_2l'_1} . \tag{2.24}$$

We rewrite Eq. (2.23) by introducing an operator Ξ,

$$\Xi_{ij}(r,y)=\int \Omega_i(r,x)[u_i(y)W'_{ij}(y,x)u_j(x)+U_{ij}(x,y)]x^2\,dx , \tag{2.25}$$

so that Eq. (2.23) becomes

$$\phi_{ia}(r)=\frac{F_l(k_i r)}{r}\delta_{ia}-\sum_{j\in P}\int\{\Omega_i(r,y)[V_{ij}(y)-(e^2/y)\delta_{ij}]+\Xi_{ij}(r,y)\}\phi_{ja}(y)y^2dy . \tag{2.26}$$

Equation (2.26) is one of a coupled set of integral equations. They are to be converted into a matrix equation through the introduction of a coordinate grid, whose points are denoted r_m, and a set of quadrature weights ρ_m. The result of this conversion has the form

$$\sum_{j,n}(\delta_{ij}\delta_{mn}+B_{im,jn})\phi_{ja}(r_n)=\frac{1}{r_m}F_{l_1}(k_i r_m)\delta_{ia} . \tag{2.27}$$

In this equation

$$B_{im,jn}=r_n^2\rho(r_n)\left[\Omega_i(r_m,r_n)\left[V_{ij}(r_n)-\frac{e^2\delta_{ij}}{r_n}\right]+\Xi_{ij}(r_m,r_n)\right] . \tag{2.28}$$

It is convenient, in considering these equations, to introduce combined indices $I=(i,m)$, $J=(j,n)$ and to arrange elements so that for each grid point, the channels follow in order. Then $B_{im,jn}$ becomes B_{IJ}; F and ϕ are matrices with columns designated by the channel of incidence (a). Then with all indices suppressed, Eq. (2.27) is simply

$$(I+B)\phi=F' . \tag{2.29}$$

The factor $1/r_m$ in Eq. (2.27) has been included in F':

$$F'_I=(1/r_m)F_{l_1}(k_i r_m)\delta_{ia} . \tag{2.30}$$

The solution of Eq. (2.29) is just

$$\phi=(I+B)^{-1}F' . \tag{2.31}$$

After ϕ has been determined on the grid of points, the K matrix is determined by fitting the solution at large distances to the prescribed asymptotic form

$$\phi_{ia}(r)\to\frac{1}{k_i^{1/2}r}[F_{l_1}(k_i r)\delta_{ia}+K_{ia}G_{l_1}(k_i r)] . \tag{2.32}$$

The large-distance behavior of the functions F and G was specified in Eq. (2.17). Although the K matrix is complex, the S matrix and the cross sections can be computed from K in the usual way,

$$S=\frac{1+iK}{1-iK} . \tag{2.33}$$

III. NUMERICAL METHODS

We will describe here briefly the essential features of the numerical methods with which the formal discussion of the proceeding section has been implemented. A more complete account will be published elsewhere.[16]

An essential feature which strongly influences the accuracy obtainable with a linear-algebraic method is the algorithm used for numerical integration. We believe this matter has been given insufficient attention in the past. The point is that there is a derivative discontinuity in the function $\Omega(r,x)$ which enters into both Eqs. (2.25) and (2.28). Such discontinuities also occur in the functions $U_{ij}(x,y)$ and $W'_{ij}(x,y)$ which enter into the construction of Ξ_{ij} [Eq. (2.25)]. If the algorithm for numerical integration does not take account of these discontinuities, the accuracy obtained will be significantly reduced. We have demonstrated this to occur in specific, simple examples in Ref. 16.

It is desirable that the derivative discontinuities should occur on the mesh points of the grid, since this enables the integration weights to be adjusted properly to take ac-

count of the discontinuities. This consideration suggests that Gaussian quadratures are not optimal in this problem, and argues in favor of the use of Newton-Cotes—type formulas with a mesh that is regular except for occasional jumps in the grid spacing. Our procedure is based on a five-point Newton-Cotes quadrature in which the error is proportional to h^6. This enables us to obtain a rather high degree of accuracy with a modest number of mesh points. Details are described in Ref. 16. However, there is an upper limit to the mesh spacing that can be used in our approach which is set by the oscillations of wave functions in the asymptotic region. Therefore, it is necessary to use a finer mesh at large distance at high incident energies than at lower energies.

There is an additional complication which arises from the existence of long-range forces. Because of the degeneracy of the levels of the hydrogenic system with respect to l for a given n, there are off-diagonal terms proportional to $1/r^2$, $1/r^3$, etc., in K_{ij}, Eq. (2.7). Analogous terms appear in U_{ij}, which because $U(x,y)$ becomes sharply peaked at $x=y$ for large x,y, give rise to an effective polarization interaction proportional to $1/r^4$ at large r. The result of this is that the K matrix cannot be determined accurately by matching the solutions to spherical Bessel functions (or Coulomb functions in the case of ions) at moderate values of r. We must use either more exact asymptotic functions which take account of the long-range interactions or, as is done in this case, carry the calculations out to large values of r. This is reasonably simple because exchange is negligible and the optical potential may be regarded as diagonal (with respect to coordinates) in this region. We have followed here the procedure of Henry *et al.*[12] for propagating K matrices as incorporated in their program ASYM3.

The optical potential calculations have been made including values of the total angular momentum $L \leq 5$ at low energies, $k^2 < 1.4$, and $L \leq 6$ for higher energies. Contributions from higher angular momenta are included approximately using the unitarized Born approximation with exchange (UBX). However, a model polarization potential described in Ref. 13 is used to determine the $1s$-$1s$ element of the K matrix. Further discussion of the UBX method for the treatment of large L can be found in Ref. 9.

IV. PSEUDOSTATE BASIS

The present calculation is based on the 18-state pseudostate basis described in Ref. 17. It contains 7 s states, 5 p states, 3 d states, 2 f states, and 1 g state, of which 7 ($1s$, $2s$, $3s$, $2p$, $3p$, and $4f$) are exact atomic states and 11 are pseudostates. A given state is denoted as

$$u_j^{(l)}(r) = \sum_k c_{jk}^{(l)} r^{n_k} e^{-\zeta_k r} \tag{4.1}$$

in which j is the state number of l is the angular momentum. The parameters and energies of this set are listed in Table I.

This set contains the exact atomic states through $n=3$ and therefore may be used to discuss elastic scattering and transitions among these states. It is evident from the energies given in the table, and this is readily confirmed by a calculation of overlaps, that the set contains good approximations to the $4s$, $4p$, and $4d$ state (plus the exact $4f$). It should therefore be possible to obtain reasonable results for elastic scattering from the states in the $n=3$ manifold.

TABLE I. Parameters and energies (in Ry) of the pseudostate basis. Note that the energies refer to the combination, Eq. (4.1), rather than to the individual components.

n_k	ζ_k	E_k
	$l=0$	
0	1.0	−1.0
0	0.5	−0.25
1	0.5	−0.111 111
0	1/3	−0.062 38
1	1/3	−0.017 23
2	1/3	0.195 88
0	0.2	2.039 64
	$l=1$	
1	1.0	−0.25
1	0.5	−0.111 111
1	1/3	−0.062 19
2	1/3	+0.027 44
1	0.2	0.909 12
	$l=2$	
2	0.5	−0.111 11
2	1/3	−0.062 45
2	0.2	+0.041 87
	$l=3$	
3	0.5	−0.0625
3	0.25	+0.033 13
	$l=4$	
4	0.4	0.0

We use this set in the following way. The states through $n=3$ are placed in the P space, the remaining twelve, which are orthogonal to them, define the Q space. The assumption is made here that these 12 states are complete enough to permit sufficiently accurate evaluation of the optical potential.

V. RESULTS

The calculations described below are based on the 18-state basis described in the previous section. In these calculations, the P space consisted of the exact atomic eigenstates through $n=3$; hence we have six-state close coupling (with exchange) supplemented by an optical potential approximately representing higher bound and continuum states. The present calculations are similar to those reported by Bransden and collaborators (BSSR), Ref. 2; the most significant differences being our use of a larger six-state basis in P space, and also a larger 12-state basis in Q space. We shall first consider elastic scattering from ground-state atoms.

TABLE II. Integrated cross section for elastic scattering from the ground state (units πa_0^2) at selected energies: *OP*, present calculation; *VAR*, Ref. 9.

k^2	$\sigma(OP)$	$\sigma(VAR)$
0.91	5.841	5.749
1.10	4.692	4.694
1.44	3.408	3.429
1.96	2.394	2.337
2.25	2.034	1.960
2.57	1.708	1.643
4.00	0.963	0.920
5.00	0.701	
7.35	0.441	

A. 1*s* elastic integrated cross sections

Our results for the integrated elastic scattering cross sections are listed in Table II at nine energies. Numerical results from a recent variational pseudostate calculation,[9] using an 11-state basis are presented for comparison. The agreement is quite good, especially in the lower part of the energy range. At higher energies, there are discrepancies of the order of 4%. Elastic scattering amplitudes through $L=5$ are presented in Table III so that others interested in optical-potential calculations will have specific numbers for comparison purposes. These amplitudes are probably not as accurate in a fundamental sense as those of Ref. 9 (the latter also agree more satisfactorily for $L=0$ with the complex energy extrapolation of McDonald and Nuttall).[18]

Our elastic cross sections are also shown in Fig. 1 in order to facilitate comparison with the results of other groups who have reported calculations using related methods. Specifically, these include three-state close coupling;[19] a two-channel calculation including the 1*s* state and a single *p* pseudostate,[20] an *R*-matrix calculation with several pseudostates,[21] and two previous optical-potential calculations.[1,7] In a qualitative sense, the agreement is quite good. The three-state close-coupling cross sections are roughly 15—20% lower than those obtained from more sophisticated calculations. Calculations including only a single polarization pseudostate[20] make a significant

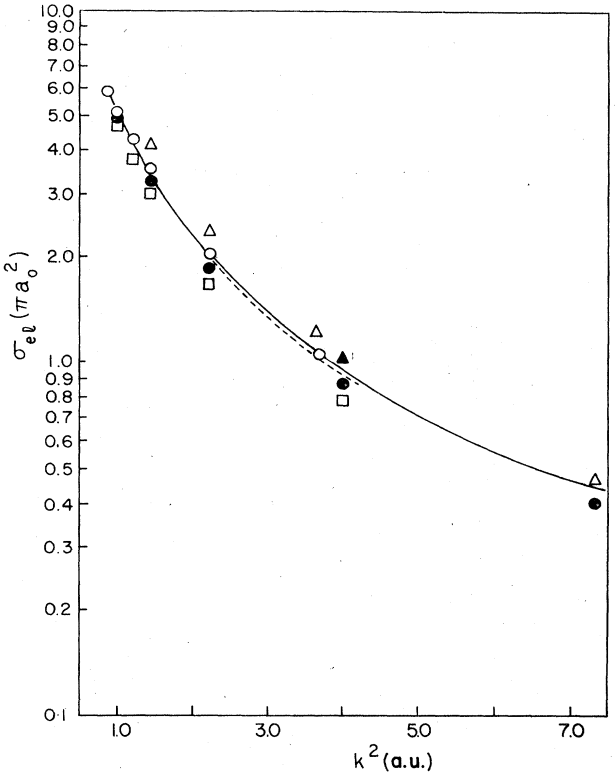

FIG. 1. Integrated cross section for elastic scattering from ground-state hydrogen (units πa_0^2). Present results, solid line; Ref. 9, dashed line. Other symbols are the following: open squares, Ref. 19; solid circles, Ref. 20; open circles, Ref. 21; open triangles, Ref. 1; solid triangles, Ref. 7.

increase. The present results are in rather good agreement with the most recent *R*-matrix calculations of Fon *et al.*[21] Some optical-potential calculations previously reported[1,7] tend to yield larger cross sections. This is a fairly significant effect ($\sim$20%) near 20 eV in regard to the work of Scott and Bransden.[1] The agreement with the calculation of BSSR[2] is within 5% (ours are lower) at 54 and 100 eV.

Unfortunately, there are no experimental measurements of the integrated elastic cross section of sufficient accura-

TABLE III. 1*s* elastic scattering amplitudes at five energies (*R* denotes seal part; *I*, imaginary part).

k^2	1.10		1.44		2.25		4.00		7.35	
	R	*I*	*R*	*I*	*R*	*I*	*R*	*I*	*R*	*I*
^1S	0.370	0.431	0.344	0.384	0.367	0.369	0.368	0.350	0.393	0.304
^3S	0.164	0.963	0.266	0.902	0.379	0.766	0.433	0.585	0.442	0.418
^1P	0.028	0.050	0.047	0.074	0.072	0.095	0.130	0.092	0.182	0.088
^3P	0.371	0.204	0.359	0.198	0.345	0.191	0.308	0.168	0.276	0.134
^1D	0.094	0.075	0.061	0.094	0.054	0.077	0.059	0.069	0.085	0.050
^3D	0.109	0.020	0.125	0.031	0.150	0.058	0.149	0.040	0.147	0.060
^1F	0.048	0.011	0.054	0.026	0.044	0.045	0.039	0.047	0.046	0.038
^3F	0.044	0.011	0.052	0.015	0.067	0.025	0.076	0.040	0.080	0.038
^1G	0.023	0.002	0.030	0.008	0.032	0.023	0.027	0.032	0.028	0.029
^3G	0.023	0.003	0.029	0.007	0.035	0.016	0.041	0.026	0.046	0.027
^1H	0.013	0.001	0.017	0.003	0.022	0.012	0.021	0.022	0.019	0.023
^3H	0.013	0.001	0.017	0.003	0.022	0.010	0.025	0.018	0.028	0.021

cy to distinguish between these theories. Calculations using coupled-state expansions have tended to produce larger cross sections as the basis set is improved. This tendency is clearly apparent in Fig. 1. There may be reason to believe that this process has converged to within 2% or 3% of the correct values below, say, 30 eV.[9] If so, the optical-potential study of Ref. 1 has definitely produced too large cross sections.

B. Elastic differential cross section

Rather high-quality experimental differential cross sections for elastic scattering are available. Figure 2 shows the comparison between our results at $k^2=0.91$, 1.44, and 1.96 (corresponding to 12.4, 19.6, and 26.7 eV) and experimental values reported in Ref. 13. (In the case $k^2=0.91$, our results are compared with measurements at 12.0 eV incident energy.) We have not shown here differential cross sections at higher energies (50 and 100 eV), because we have not yet included enough partial waves to obtain converged results at large angles. Numerical values for these differential cross sections are given in Table IV. In general, the agreement between theory and experiment is quite good, and in fact is superior to that obtained in the calculations reported in Ref. 13.

TABLE IV. $1s$ elastic differential cross section (units $a_0^2\mathrm{sr}^{-1}$).

Angle (deg)	k^2 0.91	1.44	1.96
0	10.00	9.74	9.53
10	7.47	6.67	6.06
20	5.42	4.30	3.56
30	3.90	2.73	2.06
40	2.82	1.76	1.23
50	2.07	1.19	0.786
60	1.56	0.845	0.538
70	1.21	0.626	0.385
80	0.981	0.482	0.284
90	0.829	0.388	0.218
100	0.739	0.328	0.178
110	0.695	0.288	0.153
120	0.685	0.262	0.135
130	0.699	0.245	0.122
140	0.730	0.236	0.111
150	0.769	0.230	0.105
160	0.809	0.225	0.101
170	0.838	0.221	0.100
180	0.848	0.219	0.100

C. Spin asymmetry in elastic scattering

Fletcher *et al.*[14] have reported values for the spin asymmetry in elastic scattering at the (single) angle of 90° at energies up to 30 eV. The specific quantity they consider is

$$A=\frac{1-r}{1+3r}\,, \tag{5.1}$$

where

$$r=|f_s(\Theta)|^2/|f_t(\Theta)|^2\,, \tag{5.2}$$

and f_s and f_t are the singlet and triplet scattering amplitudes. They reported that a discrepancy existed between their experiments and results of variational pseudostate calculations.[13] However, in their determination of the value of A attributed to the pseudostate calculations, they included only the partial waves of $L=0$ and 2 (odd L partial waves do not contribute at a scattering angle of 90°). Our values for A include larger values of L as discussed at the end of Sec. III.

Our results for A are presented in Fig. 3 where they are compared with the experimental values. The discrepancy reported in Ref. 14 has been removed. Numerical values for A, and additional discussion of this quantity may be found in Ref. 22.

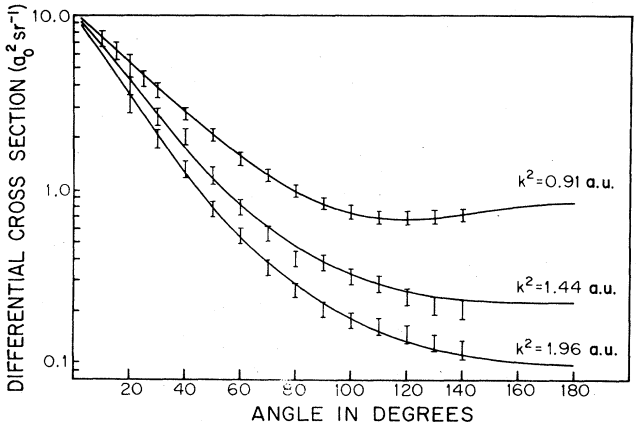

FIG. 2. $1s$ elastic differential cross sections (units $a_0^2\mathrm{sr}^{-1}$). Curves are labeled by the value of k^2. Experimental values are from Ref. 13.

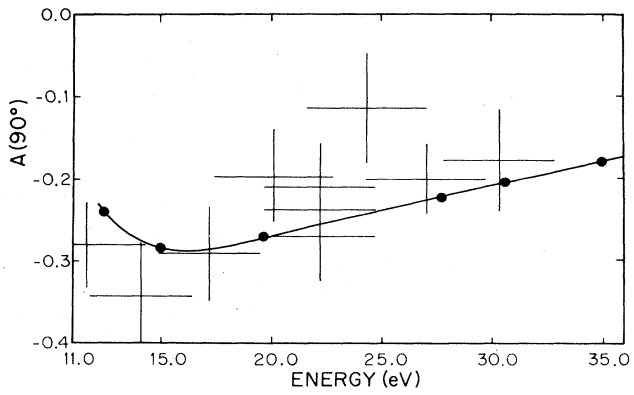

FIG. 3. Spin asymmetry parameter A for $1s$ elastic scattering. The experimental results are from Ref. 14.

D. Excitation of $n=2$ states

Our results for the integrated cross sections for excitation of the $2s$ and $2p$ states are shown graphically in Figs. 4 and 5, where they are compared with the variational pseudostate results of Ref. 9, and with three-state close-coupling results.[19,23] The present results in the case of elastic scattering were in quite good agreement with those of the most elaborate pseudostate calculations but this is not the situation for excitation, where the disagreements are quite significant, and exceed the estimated error ($\sim 10\%$) of the results of Ref. 9. It will be observed, however, that the present results are much closer to those of Ref. 9 than to those obtained from three-state close coupling. The latter disagree with the variational results by more than a factor of 2 near 20 eV for $2s$ excitation, and by just under a factor of 2 for $2p$ excitation.

The optical-potential procedure, as we have implemented it, is certainly approximate. Second-order exchange is neglected, as are all terms in the optical potential of higher than second order. Evidently the omitted terms have little effect on elastic scattering but a significant effect on excitation. But there has certainly been a substantial improvement over three-state close coupling. Limited-basis-set close-coupling calculations represent the "state of the art" for atoms and ions more complex than hydrogen. Although results from an optical-potential calculation cannot be expected to be exact, we believe that the use of optical-potential methods would lead to improved results for excitation for other systems.

E. Total cross section

We can determine the total cross section from the imaginary part of the elastic scattering amplitude with the use of the optical theorem

$$\sigma_T=\frac{1}{k^2}\sum_{L,S}(2L+1)(2S+1)\mathrm{Im}(f_{L,S})\ , \tag{5.3}$$

where $f_{L,S}$ is the scattering amplitude for total angular momentum L and spin S. The factors $(2L+1)(2S+1)$ lead to relatively slow convergence of the sum at higher energies where many partial waves contribute. The UBX (unitarized Born with exchange) which has been used for rapid but rough estimation of the higher-partial-wave contributions of excitation is numerically unreliable in this case because it neglects ionization. For this reason, we give here our values for the total cross section only at $k^2=0.91$, 1.10, and 1.44 where a reasonable degree of convergence is attained. The maximum value of L included in (5.3) is listed in Table V. Results obtained similarly from the variational calculation of Ref. 10 are included for comparison. A very rough estimate based on assuming that the rate of convergence of UBX calculations with L may also apply in the present situation suggest that the higher L contribution is probably almost negligible (~ 0.01) at $k^2=0.91$ but may be as much as 5% (~ 0.2) at $k^2=1.44$. The agreement between the present optical-model calculations and the previous variational results is quite reasonably good (within about 5%), suggesting we are probably able to obtain reasonable values for

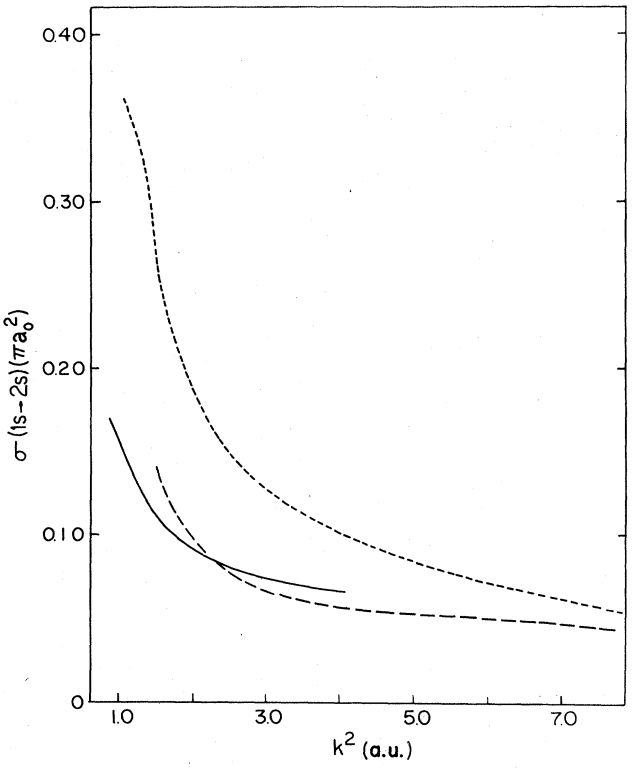

FIG. 4. Integrated cross section for $2s$ excitation: long-dashed line, present results; solid line, variational pseudostate calculation; short-dashed line, three-state close coupling.

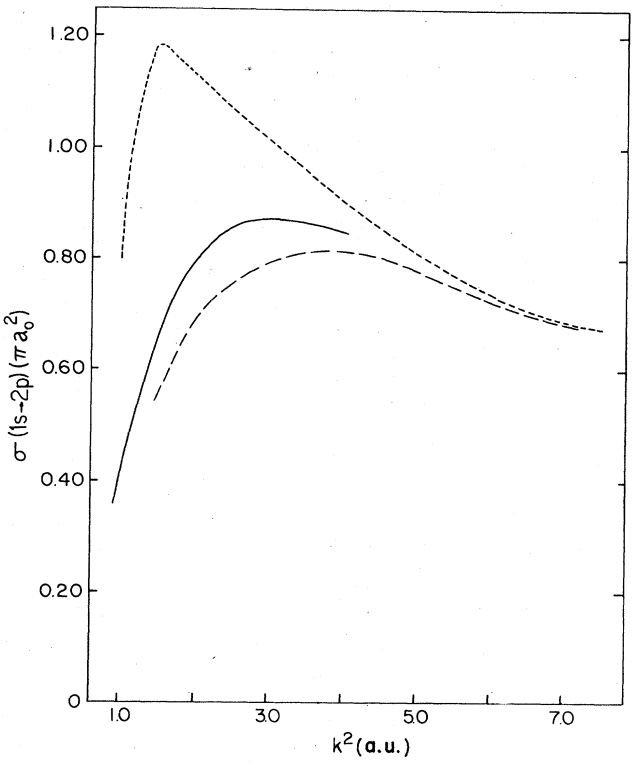

FIG. 5. Similar to Fig. 4 for $2p$ excitation.

TABLE V. Total cross section (units πa_0^2) as obtained from this calculation and from the variational pseudostate calculation of Ref. 10: *OP*, present calculation; *VAR*, Ref. 9. L_{max} is the largest value of the total angular momentum included.

k^2	L_{max}	$\sigma(OP)$	$\sigma(VAR)$
0.91	5	6.48	6.41
1.10	5	5.86	5.56
1.44	6	4.85	4.74

σ_T from the optical model. Our value for σ_T near 20 eV is roughly 25% smaller than that obtained by Scott and Bransden,[1] which we believe to be an overestimate.

VI. CONCLUSIONS

We have developed and tested a procedure by which a pseudostate expansion is used to determine an optical-potential matrix, which is then used in close-coupling calculations of scattering. The present application concerns electron-hydrogen scattering. In this context, our present work can be viewed as six-state close-coupling with exchange, supplemented by an optical potential derived from twelve additional states. Our results for elastic scattering from the ground state appear to be quite accurate and resolve a discrepancy between theory and experiment in regard to the spin asymmetry in elastic scattering at 90°. The results for excitation do not appear to be as accurate as those for elastic scattering, but do offer a substantial improvement over conventional close coupling. Good values for the total cross section are obtained. We contemplate future calculations involving scattering from excited states of hydrogen and hydrogenic ions, and the application of this method to more complex atoms and ions.

ACKNOWLEDGMENT

This work was supported in part by the National Bureau of Standards, U.S. Department of Commerce.

[1] T. Scott and B. H. Bransden, J. Phys. B **14**, 2277 (1981).
[2] B. H. Bransden, T. Scott, R. Shingal, and R. K. Roychoudhury, J. Phys. B **15**, 4605 (1982).
[3] B. H. Bransden and A. T. Stelbovics, J. Phys. B **17**, 1877 (1984).
[4] I. E. McCarthy and A. T. Stelbovics, Phys. Rev. A **22**, 502 (1980).
[5] I. E. McCarthy and A. T. Stelbovics, Phys. Rev. A **28**, 2963 (1983).
[6] B. H. Bransden, I. E. McCarthy, J. D. Mitroy, and A. T. Stelbovics, Phys. Rev. A **32**, 166 (1985).
[7] J. Callaway, Adv. Phys. **29**, 771 (1980).
[8] P. G. Burke, K. A. Berrington, and C. V. Sukumar, J. Phys. B **14**, 289 (1981).
[9] J. Callaway, Phys. Rev. A **32**, 775 (1985).
[10] L. A. Collins and B. I. Schneider, Phys. Rev. A **24**, 2387 (1981).
[11] L. A. Collins and B. I. Schneider, Phys. Rev. A **27**, 101 (1983).
[12] R. J. W. Henry, S. P. Rountree, and E. R. Smith, Comput. Phys. Commun. **23**, 233 (1981).
[13] J. Callaway and J. F. Williams, Phys. Rev. A **12**, 2312 (1975).
[14] G. D. Fletcher, M. J. Alguard, T. J. Gay, V. W. Hughes, P. F. Wainwright, M. S. Lubell, and W. Raith, Phys. Rev. A **31**, 2854 (1985).
[15] I. E. Percival and M. J. Seaton, Proc. Cambridge Philos. Soc. **53**, 654 (1957).
[16] D. H. Oza and J. Callaway, J. Comput. Phys. (to be published).
[17] J. Callaway, Phys. Rep. **45**, 89 (1978).
[18] F. A. McDonald and J. Nuttall, Phys. Rev. A **4**, 1821 (1971).
[19] P. G. Burke, H. M. Schey, and K. Smith, Phys. Rev. **129**, 1258 (1963).
[20] W. C. Fon, P. G. Burke, and A. E. Kingston, J. Phys. B **11**, 521 (1978).
[21] W. C. Fon, K. A. Berrington, P. G. Burke, and A. E. Kingston, J. Phys. B **14**, 1041 (1981).
[22] D. H. Oza and J. Callaway, Phys. Rev. A **32**, 2534 (1985).
[23] A. E. Kingston, W. C. Fon, and P. G. Burke, J. Phys. B **9**, 605 (1976).